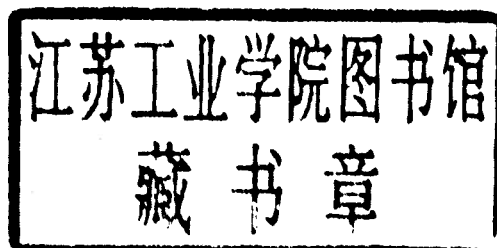


PROGRESS IN THERMAL BARRIER COATINGS

**The
American
Ceramic
Society**



Progress in Thermal Barrier Coatings



 **WILEY**

A John Wiley & Sons, Inc., Publication

Copyright © 2009 by The American Ceramic Society. All rights reserved.

Published by John Wiley & Sons, Inc., Hoboken, New Jersey.

Published simultaneously in Canada.

No part of this publication may be reproduced, stored in a retrieval system, or transmitted in any form or by any means, electronic, mechanical, photocopying, recording, scanning, or otherwise, except as permitted under Section 107 or 108 of the 1976 United States Copyright Act, without either the prior written permission of the Publisher, or authorization through payment of the appropriate per-copy fee to the Copyright Clearance Center, Inc., 222 Rosewood Drive, Danvers, MA 01923, (978) 750-8400, fax (978) 750-4470, or on the web at www.copyright.com. Requests to the Publisher for permission should be addressed to the Permissions Department, John Wiley & Sons, Inc., 111 River Street, Hoboken, NJ 07030, (201) 748-6011, fax (201) 748-6008, or online at <http://www.wiley.com/go/permission>.

Limit of Liability/Disclaimer of Warranty: While the publisher and author have used their best efforts in preparing this book, they make no representations or warranties with respect to the accuracy or completeness of the contents of this book and specifically disclaim any implied warranties of merchantability or fitness for a particular purpose. No warranty may be created or extended by sales representatives or written sales materials. The advice and strategies contained herein may not be suitable for your situation. You should consult with a professional where appropriate. Neither the publisher nor author shall be liable for any loss of profit or any other commercial damages, including but not limited to special, incidental, consequential, or other damages.

For general information on our other products and services or for technical support, please contact our Customer Care Department within the United States at (800) 762-2974, outside the United States at (317) 572-3993 or fax (317) 572-4002.

Wiley also publishes its books in a variety of electronic formats. Some content that appears in print may not be available in electronic format. For information about Wiley products, visit our web site at www.wiley.com.

Library of Congress Cataloging-in-Publication Data is available.

ISBN 978-0-470-40838-4

Printed in the United States of America.

10 9 8 7 6 5 4 3 2 1

Introduction

Ceramics are used to coat other materials, usually metals, to protect them from high temperatures, moisture, oxygen, wear, corrosive fluids and body fluids. Thermal barrier coatings (TBCs) have their greatest application in protecting metal parts used in heat engines. The metal parts have the strength required for heat engine operation; however, they cannot withstand the high temperatures necessary for efficient and clean operation of the heat engine. TBCs provide this protection.

This edition of Progress in Ceramic Technology series is a compilation of articles published on TBCs by The American Ceramic Society (ACerS). These publications include the *American Ceramic Society Bulletin*, *Journal of the American Ceramic Society*, *International Journal of Applied Ceramic Technology*, *Ceramic Engineering and Science Proceedings* (CESP) and *Ceramic Transactions* (CT).

Papers in this edition are divided into five categories: Applications, Material Improvements and Novel Compositions, Developments in Processing, Testing and Characterization, Mechanical Properties, and Thermal Properties. The publication citations are included after each title in the table of contents.

Other articles on thermal barrier coatings can be located by searching the Society's website at www.ceramics.org.

Contents

Introduction	xi
APPLICATIONS	
Corrosion Resistant Thermal Barrier Coating Materials for Industrial Gas Turbine Applications Michael D. Hill, Davin P. Phelps, and Douglas E. Wolfe <i>CESP</i> , Vol. 29, Is. 4, 123-132, 2008	3
Industrial Sensor TBCs: Studies on Temperature Detection and Durability X. Chen, Z. Mutasim, and J. Price, J. P. Feist, A. L. Heyes and S. Seefeldt <i>Int. J. of Appl. Ceram. Technol.</i> , Vol. 2, No. 5, p. 414-421, 2005	13
Industrial TBCs A. Kulkarni and H. Herman <i>Am. Ceram. Soc. Bull.</i> , Vol. 83, No. 6, p. 9801-9804, 2004	21
Low Thermal Conductivity Ceramics for Turbine Blade Thermal Barrier Coating Application U. Schulz, B. Saint-Ramond, O. Lavigne, P. Moretto, A. vanLieshout, and A. Borger <i>CESP</i> , Vol. 25, No. 4, p. 375-380, 2004	25
Thermal and Environmental Barrier Coatings for SiC/SiC CMCs in Aircraft Engine Applications I. Spitsberg and J. Steivel <i>Int. J. Appl. Ceram. Technol.</i> , Vol. 1, No. 4, P. 291-301, 2004	31
Review on Advanced EB-PVD Ceramic Topcoats for TBC Applications U. Schulz, B. Saruhan, K. Fritscher, and C. Leyens <i>Int. J. Appl. Ceram. Technol.</i> , Vol. 1, No.4, p. 302-314, 2004	43
MATERIAL IMPROVEMENTS AND NOVEL COMPOSITIONS	
Corrosion Behavior of New Thermal Barrier Coatings R. Vaßen, D. Sebold, and D. Stöver <i>CESP</i> , Vol. 28, No. 3, p. 27-38, 2007	59
Thermal Conductivity of Plasma-Sprayed Aluminum Oxide—Multiwalled Carbon Nanotube Composites Srinivas R. Bakshi, Kantesh Balani, Arvind Agarwal <i>J. Am. Ceram. Soc.</i> Vol. 91, No. 3, 942-947, 2008	71
Infiltration-Inhibiting Reaction of Gadolinium Zirconate Thermal Barrier Coatings with CMAS Melts S. Krämer, J. Yang, and C. Levi <i>J. Am. Ceram. Soc.</i> , Vol. 91, No. 2, p. 576-583, 2008	77
Segmentation Cracks in Plasma Sprayed Thin Thermal Barrier Coatings H. Guo, H. Murakami, and S. Kuroda <i>CESP</i> , Vol. 27, No. 3, p. 17-27, 2007	85

Design of Alternative Multilayer Thick Thermal Barrier Coatings H. Samadi and T. Coyl <i>CESP</i> , Vol. 27, No. 3, p. 29-35, 2007	97
Lanthanum-Lithium Hexaaluminate—A New Material for Thermal Barrier Coatings in Magnetoplumbite Structure—Material and Process Development G. Pracht, R. Vaßen and D. Stöver <i>CESP</i> , Vol. 27, No. 3, p. 87-99, 2007	105
Thermal Barrier Coatings Design with Increased Reflectivity and Lower Thermal Conductivity for High-Temperature Turbine Applications M. Kelly, D. Wolfe, J. Singh, J. Eldridge, D-M Zhu, and R. Miller <i>Int. J. Appl. Ceram. Technol.</i> , Vol. 3, No. 2, p. 81-93, 2006	119
Delamination-Indicating Thermal Barrier Coatings Using YSZ:Eu Sublayers J. Eldridge, T. Bencic, C. Spuckler, J. Singh, and D. Wolfe <i>J. Am. Ceram. Soc.</i> , Vol. 89, No. 10, p. 3246-3251, 2006	133
Erosion-Indicating Thermal Barrier Coatings Using Luminescent Sublayers J. Eldridge, J. Singh, and D. Wolfe <i>J. Am. Ceram. Soc.</i> , Vol. 89, No. 10, p. 3252-3254, 2006	139
Rare-Earth Zirconate Ceramics with Fluorite Structure for Thermal Barrier Coatings Q. Xu, W. Pan, J. Wang, C. Wan, L. Qi, H. Miao, K. Mori, and T. Torigoe <i>J. Am. Ceram. Soc.</i> , Vol. 89, No. 1, p. 340-342, 2006.	143
Co-Doping of Air Plasma-Sprayed Yttria- and Ceria-Stabilized Zirconia for Thermal Barrier Applications Z. Chen, R. Trice, H. Wang, W. Porter, J. Howe, M. Besser and D. Sordélet <i>J. Am. Ceram. Soc.</i> , Vol. 88, No. 6, p. 1584-1590, 2005	147
Ta ₂ O ₅ /Nb ₂ O ₅ and Y ₂ O ₃ Co-doped Zirconias for Thermal Barrier Coatings S. Raghavan, H. Wang, R. Dinwiddie, W. Porter, R. Vassen, D. Stover, and M. Mayo <i>J. Am. Ceram. Soc.</i> , Vol. 87, No. 3, p. 431-37, 2004	155
New Thermal Barrier Coatings Based on Pyrochlore/YSZ Double-Layer Systems R. Vaßen, F. Traeger, and D. Stöver <i>Int. J. Appl. Ceram. Technol.</i> , Vol. 1, No. 4, p. 351-361, 2004	163
Development of Advanced Low Conductivity Thermal Barrier Coatings D. Zhu and R. Miller <i>Int. J. Appl. Ceram. Technol.</i> , Vol. 1, No. 1, p. 86-94, 2004	175
DEVELOPMENTS IN PROCESSING	
Process and Equipment for Advanced Thermal Barrier Coatings Albert Feuerstein, Neil Hitchman, Thomas A. Taylor, and Don Lemen <i>CESP</i> , Vol. 29, Is. 4, 107-122, 2008	187
Influence of Porosity on Thermal Conductivity and Sintering in Suspension Plasma Sprayed Thermal Barrier Coatings H. Kaßner, A. Stuke, M. Rödiger, R. Vaßen, and D. Stöver <i>CESP</i> , Vol. 29, Is. 4, 147-158, 2008	203
Thermal and Mechanical Properties of Zirconia/Monazite-Type LaPO ₄ Nanocomposites Fabricated by PECS S-H Kim, T. Sekino, T. Kusunose, and A. Hirvonen <i>CESP</i> , Vol. 28, Is. 3, p. 19-26, 2007	215
Dense Alumina-Zirconia Coatings Using the Solution Precursor Plasma Spray Process D. Chen, E. Jordan, M. Gell, and X. Ma <i>J. Am. Ceram. Soc.</i> , Vol. 91, No. 2, p. 359-365, 2008	223

Thermal Stability of Air Plasma Spray and Solution Precursor Plasma Spray Thermal Barrier Coatings D. Chen, M. Gell, E. Jordan, E. Cao, and X. Ma <i>J. Am. Ceram. Soc.</i> , Vol. 90, No. 10, p. 3160-3166, 2007	231
Mechanical Design for Accommodating Thermal Expansion Mismatch in Multilayer Coatings for Environmental Protection at Ultrahigh Temperatures Jie Bai, Kurt Maute, Sandeep R. Shah and Rishi Raj <i>J. Am. Ceram. Soc.</i> , Vol. 90, No. 1, p. 170-176, 2007	239
Grain-Boundary Grooving of Plasma-Sprayed Yttria-Stabilized Zirconia Thermal Barrier Coatings K. Erk, C. Deschaseaux, and R. Trice <i>J. Am. Ceram. Soc.</i> , Vol. 89, No. 5, p. 1673-1678, 2006	247
Novel Deposition of Columnar $Y_3Al_5O_{12}$ Coatings by Electrostatic Spray-Assisted Vapor Deposition Y. Wu, J. Du and K-L Choy <i>J. Am. Ceram. Soc.</i> , Vol. 89, No. 1, p. 385-387, 2006	253
TESTING AND CHARACTERIZATION	
Monitoring the Phase Evolution of Yttria Stabilized Zirconia in Thermal Barrier Coatings Using the Rietveld Method G. Witz, V. Shklover, W. Steure, S. Bachegowda, and H.-P. Bossmann <i>CESP</i> , Vol. 28, No. 3, p. 41-51, 2007	259
Thermal Imaging Characterization of Thermal Barrier Coatings J. Sun <i>CESP</i> , Vol. 28, No. 3, p. 53-60, 2008	271
Examination on Microstructural Change of a Bond Coat in a Thermal Barrier Coating for Temperature Estimation and Aluminum-Content Prediction M. Okada, T. Hisamatsu, and T. Kitamura <i>CESP</i> , Vol. 28, No. 3, p. 61-69, 2008	279
Quantitative Microstructural Analysis of Thermal Barrier Coatings Produced by Electron Beam Physical Vapor Deposition M. Kelly, J. Singh, J. Todd, S. Copley, and D. Wolfe <i>CESP</i> , Vol. 28, No. 3, p. 71-80, 2008	289
Investigation of Damage Prediction of Thermal Barrier Coating Y. Ohtake <i>CESP</i> , Vol. 28, No. 3, p. 81-84, 2008	299
Corrosion Rig Testing of Thermal Barrier Coating Systems R. Vaßen, D. Sebold, G. Pracht, and D. Stöver <i>CESP</i> , Vol. 27, No. 3, p. 47-59, 2007	303
Oxidation Behavior and Main Causes for Accelerated Oxidation in Plasma Sprayed Thermal Barrier Coatings H. Arikawa, Y. Kojima, M. Okada, T. Hoshioka, and T. Hisamatsu <i>CESP</i> , Vol. 27, No. 3, p. 69-80, 2007	317
Crack Growth and Delamination of Air Plasma-Sprayed Y_2O_3 - ZrO_2 TBC After Formation of TGO Layer M. Hasegawa, Y-F Liu, and Y. Kagawa <i>CESP</i> , Vol. 27, No. 3, p. 81-85, 2007	329
Characterization of Cracks in Thermal Barrier Coatings Using Impedance Spectroscopy L. Deng, X. Zhao, and P. Xiao <i>CESP</i> , Vol. 27, No. 3, p. 191-206, 2007	335
Nondestructive Evaluation Methods for High Temperature Ceramic Coatings W. Ellingson, R. Lipanovich, S. Hopson, and R. Visher <i>CESP</i> , Vol. 27, No. 3, p. 207-214, 2007	351

Phase Evolution in Yttria-Stabilized Zirconia Thermal Barrier Coatings Studied by Rietveld Refinement of X-Ray Powder Diffraction Patterns	359
G. Witz, V. Shklover, W. Steurer, S. Bachegowda, H-P Bossmann <i>J. Am. Ceram. Soc.</i> , Vol. 90, No. 9, p. 2935-2940, 2007	
Characterization of Chemical Vapor-Deposited (CVD) Mullite+CVD Alumina+Plasma-Sprayed Tantalum Oxide Coatings on Silicon Nitride Vanes After an Industrial Gas Turbine Engine Field Test	365
J. A. Haynes, S. M. Zemskova, H. T. Lin, M. K. Ferber and W. Westphal <i>J. Am. Ceram. Soc.</i> , Vol. 89, No. 11, p. 3560-3563, 2006	
Monitoring Delamination Progression in Thermal Barrier Coatings by Mid-Infrared Reflectance Imaging	369
J. Eldridge, C. Spuckler, and R. Martin <i>Int. J. Appl. Ceram. Technol.</i> , Vol. 3, No. 2, p. 94-104, 2006	
Noncontact Methods for Measuring Thermal Barrier Coating Temperatures	381
M. Gentleman, V. Lugh, J. Nychka, and D. Clarke <i>Int. J. of Appl. Ceram. Technol.</i> , Vol. 3, No. 2, p. 105-112, 2006	
Modeling the Influence of Reactive Elements on the Work of Adhesion between Oxides and Metal Alloys	389
J. Bennett, J. M. Kranenburg and W. G. Sloof <i>J. Am. Ceram. Soc.</i> , Vol. 88, No. 8, p. 2209-2216, 2005	
Hot Corrosion Mechanism of Composite Alumina/Yttria-Stabilized Zirconia Coating in Molten Sulfate–Vanadate Salt	397
N. Wu, Z. Chen, and S. Mao <i>J. Am. Ceram. Soc.</i> , Vol. 88, No. 3, p. 675-682, 2005	
Microstructure–Property Correlations in Industrial Thermal Barrier Coatings	405
A. Kulkarni, A. Goland, Herbert Herman, A. Allen, J. Ilavsky, G. Long, C. Johnson, and J. Ruud <i>J. Am. Ceram. Soc.</i> , Vol. 87, No. 7, p. 1294-1300, 2004	
TBC Integrity	413
J. Eldridge, C. Spuckler, J. Nesbitt, and K. Street <i>Am. Ceram. Soc. Bull. Online</i> , Vol. 83, No. 6, p. 9801-9804, 2004	
Photoluminescence Piezospectroscopy: A Multi-Purpose Quality Control and NDI Technique for Thermal Barrier Coatings	417
M. Gell, S. Sridharan, M. Wen, and E. Jordan <i>Int. J. Appl. Ceram. Technol.</i> , Vol. 1, No. 4, p. 316-319, 2004	
MECHANICAL PROPERTIES	
Elastic and Inelastic Deformation Properties of Free Standing Ceramic EB-PVD Coatings	433
M. Bartsch, U. Fuchs, and J. Xu <i>CESP</i> , Vol. 28, No. 3, p. 11-18, 2007	
Creep Behavior of Plasma Sprayed Thermal Barrier Coatings	441
R. Soltani, T. Coyle, and J. Mostaghimi <i>CESP</i> , Vol. 27, No. 3, p. 37-46, 2007	
Simulation of Stress Development and Crack Formation in APS-TBCS for Cyclic Oxidation Loading and Comparison with Experimental Observations	451
R. Herzog, P. Bednarz, E. Trunova, V. Shemet, R. Steinbrech, F. Schubert, and L. Singheiser <i>CESP</i> , Vol. 27, No. 3, p.103-114, 2007	
Numerical Simulation of Crack Growth Mechanisms Occurring Near the Bondcoat Surface in Air Plasma Sprayed Thermal Barrier Coatings	463
Casu, J.-L. Marques, R. Vassen, and D. Stover <i>CESP</i> , Vol. 27, No. 3, p. 115-126, 2007	
Damage Prediction of Thermal Barrier Coating	475
Y. Ohtake <i>CESP</i> , Vol. 27, No. 3, p. 139-146, 2007	

Creep Behavior of Plasma-Sprayed Zirconia Thermal Barrier Coatings R. Soltani, T. Coyle, and J. Mostaghimi <i>J. Am. Ceram. Soc.</i> , Vol. 90, No. 9, p. 2873-2878, 2007	483
Application of Hertzian Tests to Measure Stress–Strain Characteristics of Ceramics at Elevated Temperatures E. Sánchez-González, J. Meléndez-Martínez, A. Pajares, P. Miranda, F. Guiberteau and B. Lawn <i>J. Am. Ceram. Soc.</i> , Vol. 90, No. 1, p. 149-153, 2007	489
Effect of Sintering on Mechanical Properties of Plasma-Sprayed Zirconia-Based Thermal Barrier Coatings S. Choi, D. Zhu and R. Miller <i>J. Am. Ceram. Soc.</i> , Vol. 88, No. 10, p. 2859-2867, 2005	495
The Measurement of Residual Strains within Thermal Barrier Coatings Using High-Energy X-Ray Diffraction J. Thornton, S. Slater, and J. Almer <i>J. Am. Ceram. Soc.</i> , Vol. 88, No. 10, p. 2817-2825, 2005	505
Stress Relaxation of Compression Loaded Plasma-Sprayed 7 Wt% Y_2O_3 – ZrO_2 Stand-Alone Coatings G. Dickinson, C. Petorak, K. Bowman, and R. Trice <i>J. Am. Ceram. Soc.</i> , Vol. 88, No. 8, p. 2202-2208, 2005	515
Mechanical Properties/Database of Plasma-Sprayed ZrO_2 -8wt% Y_2O_3 Thermal Barrier Coatings S. Choi, D. Zhu, and R. Miller <i>Int. J. Appl. Ceram. Technol.</i> , Vol. 1, No. 4, p. 330-342, 2004	523
THERMAL PROPERTIES	
Thermal and Mechanical Properties of Zirconia Coatings Produced by Electrophoretic Deposition Baufeld, O. van der Beist, and H-J Ratzer-Scheibe <i>CESP</i> , Vol. 28, No. 3, p. 3-10, 2008	539
Effect of an Opaque Reflecting Layer on the Thermal Behavior of a Thermal Barrier Coating C. Spuckler <i>CESP</i> , Vol. 28, No. 3, p. 87-98, 2008	547
Optimizing of the Reflectivity of Air Plasma Sprayed Ceramic Thermal Barrier Coatings A. Stuke, R. Carius, J.-L. Marqués, G. Mauer, M. Schulte, D. Sebold, R. Vaßen, and D. Stöver <i>CESP</i> , Vol. 28, No. 3, p. 99-113, 2008	559
Thermal Conductivity of Nanoporous YSZ Thermal Barrier Coatings Fabricated by EB-PVD B-K Jang and H. Matsubara <i>CESP</i> , Vol. 28, No. 3, p. 115-123, 2008	575
Comparison of the Radiative Two-Flux and Diffusion Approximations C. Spuckler <i>CESP</i> , Vol. 27, No. 3, p.127-137, 2007	585
Relation of Thermal Conductivity with Process Induced Anisotropic Void Systems in EB-PVD PYSZ Thermal Barrier Coatings A. Flores Renteria, B. Saruhan, and J. Ilavsky <i>CESP</i> , Vol. 27, No. 3, p. 3-15, 2007	597
Thermal Properties of Nanoporous YSZ Coatings Fabricated by EB-PVD B-K Jang, N. Yamaguchi, and H. Matsubara <i>CESP</i> , Vol. 27, No. 3, p. 61-67, 2007	611
Thermochemical Interaction of Thermal Barrier Coatings with Molten CaO – MgO – Al_2O_3 – SiO_2 (CMAS) Deposits S. Krämer, J. Yang, C. Levi, and C. Johnson <i>J. Am. Ceram. Soc.</i> , Vol. 89, No. 10, p. 3167-3175, 2006	619

Applications

CORROSION RESISTANT THERMAL BARRIER COATING MATERIALS FOR INDUSTRIAL GAS TURBINE APPLICATIONS

Michael D. Hill and Davin P. Phelps.
Trans-Tech Inc.
Adamstown, MD 21710 USA

Douglas E. Wolfe.
Assist Professor, Materials Science and Engineering Department
The Pennsylvania State University
University Park, Pa 16802 USA

ABSTRACT

Thermal Barrier Coatings are ceramic materials that are deposited on metal turbine blades in aircraft engines or industrial gas turbines which allow these engines to operate at higher temperatures. These coatings protect the underlying metal superalloy from creep, oxidation and/or localized melting by serving as an insulating barrier to protect the metal from the hot gases in the engine core. While for aircraft engines, pure refined fuels are used, it is desirable for industrial gas turbine applications that expensive refining operations be minimized. However, acidic impurities such as sulfur and vanadium are common in these “dirty” fuels and will attack the thermal barrier coating causing reduced coating lifetimes and in the worse case catastrophic failure due to spallation of the coating. The industry standard coating material is stabilized zirconia with seven weight percent yttria stabilized zirconia being the most common. When used in industrial gas turbines, the vanadium oxide impurities react with the tetragonal zirconia phase causing undesirable phase transformations. Among these transformations is that from tetragonal to monoclinic zirconia. This transformation is accompanied by a volume expansion which serves to tear apart the coating reducing the coating lifetime. Indium oxide is an alternative stabilizing agent which does not react readily with vanadium oxide. Unfortunately, indium oxide is very volatile and does not readily stabilize zirconia, making it difficult to incorporate the indium into the coating. However, by pre-reacting the indium oxide with samarium oxide or gadolinium oxide to form a stable perovskite (GdInO_3 or SmInO_3) the indium oxide volatilization is prevented allowing the indium oxide incorporation into the coating. Comparison of EDX data from evaporated coatings containing solely indium oxide and those containing GdInO_3 are presented and show that the indium is present in greater quantities in those coatings containing the additional stabilizer. Corrosion tests by reaction with vanadium pentoxide were performed to determine the reaction sequence and to optimize the chemical composition of the coating material. Lastly, select x-ray diffraction phase analysis will be presented.

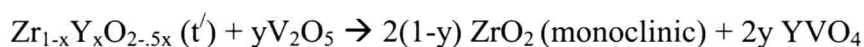
INTRODUCTION

Thermal Barrier Coatings are ceramic materials that are deposited on metal turbine blades in aircraft engines or industrial gas turbines which allow these engines to operate at higher temperatures. These coatings protect the underlying metal superalloy from creep, oxidation and/or localized melting by serving as an insulating barrier to protect the metal from the hot gases in the engine core.

Several impurities common in fuels have been identified and associated with corrosion in EB-PVD coatings. These impurities include sodium, sulfur, phosphorus and especially vanadium. These impurities react with conventional YSZ turbine blade coatings, severely limiting the coating lifetime. Therefore, it is of great interest to develop alternative materials that react less readily with fuel contaminants and therefore increase the operating lifetime of the coating.

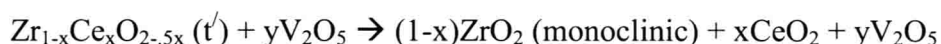
Standard 8YSZ EB-PVD coatings contain 8-weight percent yttria and crystallize in the metastable t' phase that is derived from a martensitic distortion of the “stabilized” cubic fluorite structure of zirconia. This rapidly cooled t' structure is the most desirable of all of the possible polymorphs in the yttria-zirconia system for TBC applications. Jones¹ described several mechanisms of chemical attack on 8YSZ coatings. These include chemical reaction, mineralization, bond coat corrosion and physical damage due to molten salt penetration. Of the four, only the first two mechanisms will be featured in this discussion.

Acidic species such as SO_3 and V_2O_5 have been shown to react with the yttria stabilizing the t' phase, destabilizing the Y_2O_3 - ZrO_2 by extraction of the Y_2O_3 . Of these, V_2O_5 has been determined to be the worst offender. Hamilton² and Susnitsky³ have studied the reaction mechanism in detail. The reaction:



is especially deleterious to the TBC integrity. The vanadium has been shown to leach the yttria out of the zirconia leaving the yttria deficient monoclinic phase of zirconia remaining. The large volume expansion (7%) caused by this transformation leads to the TBC spalling therefore exposing the bond coat to further chemical attack.

Mineralization, on the other hand, describes a catalytic process by which a metastable phase (in this case, the t' phase) is broken into its stable phase assemblages by a catalyst or mineralizer. For example, ceria stabilized zirconia was investigated as a corrosion resistant coating due to the fact that ceria does not react with vanadium pentoxide.



However, vanadium does act as a mineralizer, destabilizing the t' phase without reacting to form the vanadate.

Alternate stabilizers for zirconia: A large number of cationic species act to stabilize the cubic and t' phases of zirconia. Therefore, one strategy toward finding corrosion resistant coatings was to find a stabilizer that is resistant to chemical attack by vanadium pentoxide. As mentioned above, ceria was investigated but found to be subject to a mineralization reaction⁴. Previous work at NRL¹ focused on studying acidic stabilizers to zirconia since basic stabilizers such as MgO and Y_2O_3 were especially susceptible to chemical attack by acidic vanadium pentoxide. Scandia (Sc_2O_3) and indium (In_2O_3) in particular were examined in detail (Jones et. al.⁵ Sheu et. al.⁶). Of these, indium was found to be the most resistant to chemical attack by vanadium pentoxide.

Indium stabilized Zirconia as a TBC coating: Although indium stabilized zirconia shows promise due to its relative inertness in vanadia containing atmospheres, there are still significant drawbacks in its use as a TBC material. First, indium volatilizes at a lower temperature than zirconia. This results in significant challenges for applying plasma sprayed TBC's¹. Although indium stabilized zirconia coatings have been made in the t' phase (Sheu⁶), concerns about the volatility of indium oxide raise questions

about the ability of indium stabilized zirconia to form a homogeneous coatings.

In ₂ O sublimates at 600 °C	10 ⁻⁴ torr at 650°C
In ₂ O ₃ sublimates at 850 °C	10 ⁻⁴ torr at 850 °C

Jones, Reidy and Mess⁵ were able to co-stabilize zirconia with yttrium oxide and indium oxide using a sol gel process. However, no attempt was made to provide ingot feedstock of this composition for EB-PVD testing. Furthermore, the high cost (> \$300/kg) of In₂O₃ has also been a barrier for further research and development efforts.

Therefore, a logical approach was to incorporate the indium oxide into the ingot in a form that would make the indium oxide less volatile, therefore minimizing incidents of spitting, pressure fluctuations, and increase coating homogeneity while still providing enhanced corrosion resistant coating solely consisting of the t' phase. The strategy was to pre-react the indium oxide with a lanthanide oxide which forms either the LnInO₃ perovskite (La, Nd or Sm) or the hexagonal LnInO₃ (Gd or Dy). If the ingot contains zirconia and the LnInO₃ or just partially stabilized zirconia without free indium oxide, it was believed that a more homogeneous corrosion resistant coating could be deposited by electron beam physical vapor deposition (EB-PVD).

Advantages of Indate pre-cursor:

- 1) Perovskite indates (LnInO₃) are refractory compounds. The electropositive lanthanide ion (also stabilizers of the t' phase) stabilizes the In³⁺ state. It is the reduction to In¹⁺ that leads to the volatilization of In.
- 2) Multiple stabilizing ions reduce thermal conductivity. The work of R. Miller⁷ showed that TBC thermal conductivity decreases when numerous ions of different ionic sizes, valence and ionic weights are simultaneously incorporated into the zirconia as stabilizing agents. These are often referred to as oxide dopant clusters.

Lanthanide Selection: There are numerous factors that will determine the selection of the lanthanide ion accompanying the indium oxide.

- 1) Range of metastable t' phase field. Ideally one would like the largest range possible. Sasaki⁸ found the t' phase between 15 and 20-mol % In₂O₃ when quenched from temperatures above 1500°C. Ideally this phase region would accompany the In mol% alone as well as the entire range up to the (Ln + In) mole percentage.
- 2) Melting temperature of LnInO₃ compound. The more refractory the compound, the better is the performance
- 3) Acidity/basicity of lanthanide ion. If La is used, this is likely to be strongly attacked by vanadium because of its basicity. As we progress through the heavier lanthanides (left to right on periodic table), the basicity decreases.
- 4) Ionic size and weight. Y is of the ideal atomic size for decreasing the monoclinic-tetragonal transformation temperature in ZrO₂. (Sasaki⁸1993). As we move to smaller ions or larger ions this change in the transformation temperature is decreased. In addition, the greater the difference in ionic size and ionic weight between the In³⁺ and the Ln³⁺ ions, the lower the thermal conductivity (Miller⁷2004).

Phase Diagram Information: Only one ternary phase diagram exists containing any Ln_2O_3 - In_2O_3 - ZrO_2 ternary systems. That one is for $\text{Ln}=\text{Pr}$ and it was produced by Bates⁹ et.al in 1989. The compatibility relationships expressed in this diagram suggest that PrInO_3 perovskite would react with zirconia to form the $\text{Pr}_2\text{Zr}_2\text{O}_7$ pyrochlore and free indium oxide, the exact situation one should avoid. In addition, it has been shown¹⁰ that the larger lanthanide ions (La-Gd) in zirconate pyrochlores react with the thermally grown oxide to form undesirable lanthanide aluminate phases. Therefore, the authors investigated Ln ions that formed stable binary oxides of the perovskite structure with In_2O_3 but did not form the pyrochlore structure or formed the pyrochlore structure sluggishly. Like the formation of the indate perovskites, the stability of the pyrochlore phase decreases as we proceed from the light to heavy lanthanides. The lanthanides of greatest interest are therefore Sm, Gd and Dy.

Sm_2O_3	Forms $\text{Sm}_2\text{Zr}_2\text{O}_7$ pyrochlore Stable to 1800°C (Yokakawa ¹¹ 1992)	Forms SmInO_3 perovskite (Schneider, Roth and Waring ¹² 1961)
Gd_2O_3	Forms $\text{Gd}_2\text{Zr}_2\text{O}_7$ pyrochlore Stable to 1575°C (Yokakawa ¹¹ 1992)	Forms hexagonal GdInO_3 (Schneider, Roth and Waring ¹² 1961)
Dy_2O_3	Does not form $\text{Dy}_2\text{Zr}_2\text{O}_7$ pyrochlore (Pascual and Duran ¹³ 1980)	Forms hexagonal DyInO_3 Stable to 1600 C (Schneider, Roth and Waring ¹² 1961)

Lanthanides heavier than Dy do not form either the pyrochlore¹³ or binary indate phases¹². The samarium series is of interest because the indate perovskite forms and since Sm is the most electropositive ion of the lanthanide series (to prevent In^{1+} formation and volatilization); however, Sm also forms the most stable pyrochlore which is undesirable. Conversely, the dysprosium series is of interest because it does not form the pyrochlore zirconate or the perovskite structure. The hexagonal compound that does form is unstable above 1600°C. Therefore the challenge is to find a compound indium oxide precursor that will prevent indium volatilization but will not react with zirconia to form a pyrochlore and thus liberate free (and volatile) In_2O_3 .

In 2007, Mohan et. al.¹⁴ reported that in addition to forming the zircon YVO_4 phase that YSZ will react with vanadate salts below 747°C to form the zirconium pyrovanadate (ZrV_2O_7) phase. The role this phase plays in the mechanical properties of YSZ coatings containing vanadium warrants further study.

EXPERIMENTAL

LnInO_3 materials were synthesized by blending yttrium, samarium, gadolinium or dysprosium oxides (loss on ignition determined at 1300°C for all starting oxides) with indium oxide in a ball-mill with yttria-stabilized zirconia (YSZ) media at 55% solids loading without dispersants for 4h. The slurry was pan dried and calcined at 1300°C for 8h. X-ray diffraction was used to evaluate the phase purity of the material by comparing with the appropriate JCPDS cards. If the reaction was incomplete, the milling and calcinations were repeated. The fully-reacted lanthanide indate compositions were then ball-milled with YSZ media until the median particle size was 2 microns or less.

Table I. - Physical and Chemical Properties of the Fired Ingot Material

Ingot Material	Fired Density	Phase Content	Evaporation Quality
6 mole% SmInO_3	4.81 g/cc	t- ZrO_2 , m- ZrO_2 + LnInO_3	Poor - Spitting
6 mole% GdInO_3	4.85 g/cc	t- ZrO_2 , m- ZrO_2 + LnInO_3	Poor - Spitting
6 mole% DyInO_3	4.80 g/cc	t- ZrO_2 , m- ZrO_2 + LnInO_3	Extremely Poor
6 mole% SmInO_3 +3 mole% Y_2O_3	4.59 g/cc	t- ZrO_2 , m- ZrO_2 + LnInO_3	Poor – Spitting
6 mole% GdInO_3 +3 mole% Y_2O_3	4.63 g/cc	t- ZrO_2 , m- ZrO_2 + LnInO_3	Poor – Spitting

The indiate precursors were then blended with zirconia to the desired composition and formed by cold isostatic pressing into the EB-PVD ingots. The materials were heat treated between 1430 °C and 1530 °C for 10h to achieve a theoretical density between 60 and 70%. Table I shows the fired densities, the phase content and the evapoaration quality of the ingot material as a function of the chemical composition. XRD revealed the fluorite structure along with residual monoclinic zirconia and the indiate perovskites as listed in Table I.

The ingots were evaporated onto platinum aluminide coated MAR-M-247 nickel based alloy one inch diameter buttons in an industrial prototype EB-PVD coating system at Penn State University. XRD and SEM microstructures were prepared for each coating, with selectEDX presented for semi-quantitative coating chemistry analysis.

Corrosion reactivity tests were performed by reacting the coated coupons with a thin coating of vanadium pentoxide and heated to temperatures between 400 – 650 °C for 4 – 6 hours. X-ray diffraction was performed on the pre-reacted and as-reacted coating to identify any phases forming due to the reaction with vanadium pentoxide.

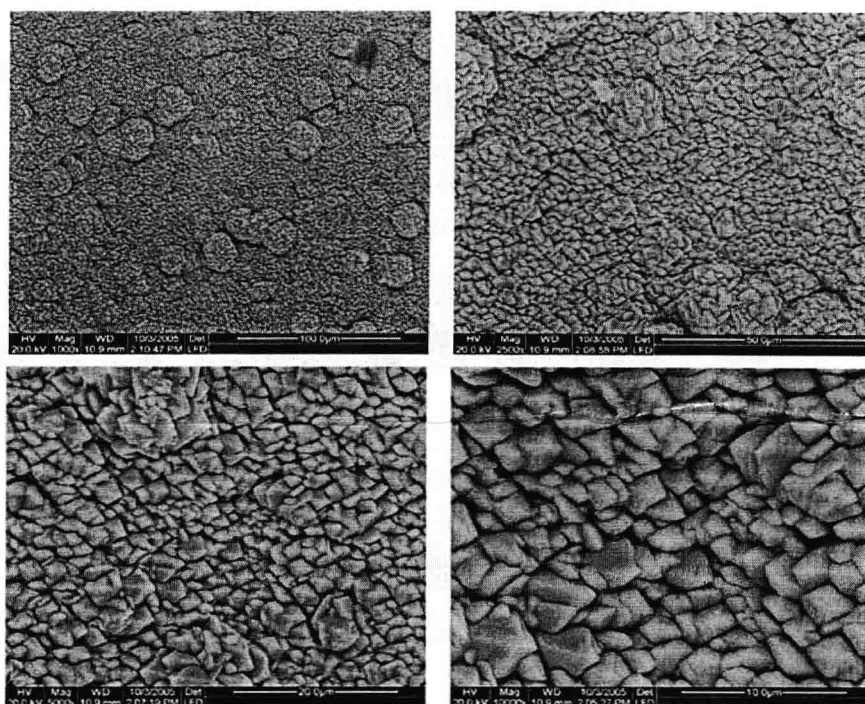
RESULTS

1) Evaporation: In general, the ingots evaporated poorly in the industrial scale EB-PVD coating unit. The material showed “spitting” and extensive cracking during evaporation. The spitting is most likely due to the difference in the vapor pressure between zirconium oxide and indium oxide containing phases in the ingot, but can also be the result of localized differences in ingot densities and degree of connected porosity. Cracking can also occur if the ingot density is too high or the ingot does not have sufficient thermal shock resistance. Despite the difficulties during ingot evaporation, coatings were obtained for each material studied. However, it should be noted that some “spits” or coating defects were observed on the surface of the coated coupons. Lastly, yttrium oxide was added into the composition as an evaporation aid during powder formulation and ingot fabrication, but it did not appear to substantially improve ingot evaporability.

2) Coating Properties: XRD revealed that all of the coatings were single phase with the desired t' structure. The coating microstructure as observed by scanning electron microscopy revealed a

columnar microstructure typical of those applied by the EB-PVD process. Figure 1 shows an SEM micrograph of the 6 mol% GdInO₃ stabilized zirconia coating surface morphology. In addition, EDX was performed on the coating surface to determine semi quantitative compositional information regarding traces of rare earth and indium oxide compositions. These results are listed in Table II.

The first measure of success was to obtain a coating which contained the acidic stabilizer In₂O₃. Table II compares the ease of evaporability and the relative amount of india within the coating for the various compositions studied. The two compositions containing samarium indate showed the highest amounts of residual indium followed by the sample containing both gadolinium and indium oxide. The ingot starting with 6 mole % indium oxide showed moderate amounts of indium remaining in the EDX trace although considerably less than either samarium containing composition despite starting with double the amount of indium oxide in the ingot.



ESEM images showing the surface morphology of ZrO₂/Y/GdInO₃ deposited on a platinum aluminide bond coated MAR-M-247 button. Sample # S050923-1H
10/4/2005

Figure 1: SEM image of surface morphology of the EB-PVD coating obtained by evaporation of the 6 mol% GdInO₃-3 mol% Y₂O₃doped zirconia ingot composition. The coatings were applied on a platinum aluminide coated nickel base alloy. The top images show a lower magnification than the bottom images

3.) Reactivity Tests: Table III shows the results of the vanadium pentoxide reactivity tests. X-ray diffraction was performed on the various coatings before and after the reactivity tests in order to determine whether the coatings reactive with vanadium oxide. If any reactions occurred, the phases were identified. The sample containing samarium indate showed only the tetragonal prime phase until